Journal of Power Sources 195 (2010) 1862–1865

Contents lists available at ScienceDirect

Journal of Power Sources

journal homepage: www.elsevier.com/locate/jpowsour

Short communication

Performance increase of microfluidic formic acid fuel cell using Pd/MWCNTs as catalyst

D. Morales-Acosta, H. Rodríguez G., Luis A. Godinez, L.G. Arriaga*

Centro de Investigación y Desarrollo Tecnológico en Electroquímica, S.C. Parque Tecnológico Querétaro Sanfandila, P.O. Box 064, Pedro Escobedo, 76703 Querétaro, Mexico

ARTICLE INFO

Article history:
Received 6 September 2009
Accepted 4 October 2009
Available online 12 October 2009

Keywords:
Microfluidic fuel cell
Formic acid
Palladium nanoparticles
Carbon nanotubes

ABSTRACT

This paper shows that the combination of an O_2 saturated acidic fluid setup (O_2-setup) and a composite of Pd nanoparticles supported on multiwalled-carbon nanotubes (Pd/MWCNTs) as anode catalyst material, results in the improvement of microfluidic fuel cell performance. Microfluidic fuel cells were constructed and evaluated at low HCOOH concentrations (0.1 and 0.5 M) using Pd/V XC-72 and Pd/MWCNTs as anode and Pt/V XC-72 as cathode electrode materials, respectively. The results show a higher power density (2.9 mW cm^{-2}) for this cell when compared to the value reported in the literature that considers a commercial Pd/V XC-72 and 3.3 mW cm^{-2} using a Pd/MWCNTs with a 50% less Pd loading than that commercial Pd/V XC-72.

1. Introduction

Recently it has reported that direct formic acid fuel cells (DFAFCs) have considerable advantages over direct methanol fuel cells (DMFCs) in portable power applications, especially in portable electronic devices (laptops computers, mobile phones, video cameras, etc.). Use of unsupported Pd as the anode catalyst in DFAFCs was first reported by Ha et al. [1]. The overall oxidation reaction at the anode is $HCOOH \rightarrow CO_2 + 2H^+ + 2e^-$ (1.45 V). Electro-oxidation of formic acid on Pd catalysts has been extensively studied; it has good electrocatalytic activity for the oxidation of formic acid which decreases CO poising effect catalysts [1–5]. Pd particles on a Vulcan XC-72® carbon support has been synthesized [1] and evaluated in DFAFC; the total power density generated per unit mass of noble metal was much higher than for the Pd black catalyst [6]. In addition to the benefits of higher palladium utilization efficiency, it was also found that the Pd/C catalysts showed less deactivation than for pure palladium during operation of the cell, especially for high concentrations of formic acid [6]. The carbon nanotube has been proposed as another support material for fuel catalysts due to its characteristics including high electron conductivity and enhanced mass transport capability and their durability in PEM fuel cells has been already tested [7]. Recently Pd/MWCNT catalyst has been synthesized by similar methods; its electrochemical activity was evaluated for formic acid oxidation by cyclic voltammetry [8,9] and the results shown a better electrocatalytic activity compared to Pd/V XC-72® [9]. Microfluidic fuel cells, sometimes called laminar flow-based fuel cells or membraneless fuel cells operate without a physical barrier; such as membrane, to separate the anode and the cathode [10]. Fuel and oxidant are introduced at the inlet of the micro-channel and the electrodes are placed at the opposite walls to complete the microfluidic fuel cell structure. Acid electrolyte present in the fuel and oxidizer streams facilitates the transverse movement of protons by diffusion from the anode to the cathode keeping low Reynolds's number *Re*. Architectures of

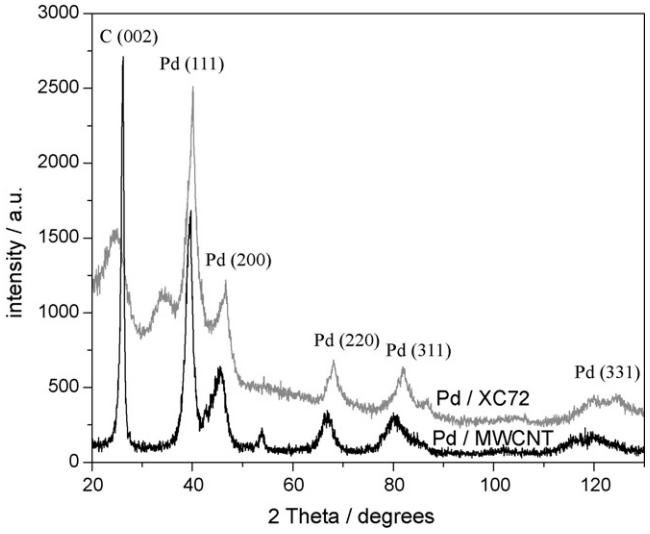

Fig. 1. XRD patterns of Pd/MWCNTs and Pd/XC-72.

* Corresponding author. Tel.: +52 442 211 6069; fax: +52 442 211 6000.
E-mail address: larriaga@cideteq.mx (L.G. Arriaga).

0378-7753/$ – see front matter © 2009 Elsevier B.V. All rights reserved.
doi:10.1016/j.jpowsour.2009.10.007

various microfluidic fuel cells were recently reviewed by Kjeang et al. [10], some of the architectures include T-channel, Y-channel or F-channel configuration. Even when the current densities obtained are satisfactory employed those configurations, the performance using dissolved oxygen in sulfuric acid (fuel: methanol, dissolved hydrogen or formic acid) tends to be mass transfer limited due to the reduced diffusivity oxygen in aqueous media (2×10^{-5} cm^2 s^{-1}) and low oxygen concentration in liquid medium. This limitation can be addressed using fluids with higher oxygen concentration like VO^{2+}/VO_2^+ [11] and potassium permanganate in sulfuric acid [12] or by integration of an air-exposed gas diffusion electrode, however some authors have reported certain scaling problems [13]. Normally the oxygen saturation stream was reached by bubbled oxygen thorough an aqueous of sulfuric acid for 20 or 30 min, in our case an O_2 saturation acidic fluid setup was incorporated with the objective of improvement in the O_2 saturation and homogenization in the acidic fluid. The following work shows the evaluation of Microfluidic fuel cell with the help of O_2-setup in low concentrations of HCOOH (0.1 and 0.5 M). The results show the highest power density (2.9 mW cm^{-2}) compare to literature [10,14,15]. Beside this we show for first time the Pd/MWCNTs as anode electrode obtaining a power density around to 3.3 mV cm^{-2} using 50% less Pd loading than commercial material (Pd/V XC-72).

2. Experimental

2.1. Pd/MWCNT catalyst synthesis

MWCNT-supported Pd electrocatalyst with a 12% metal loading was prepared by impregnation method. MWCNT support was previously synthesized utilizing the spray pyrolysis technique [16], followed by a functionalization procedure as described elsewhere [9]. MWCNTs were added to a HNO_3/H_2SO_4 (1:4, V/V) solution and stirred for 5 h at 60 °C under refluxing conditions. MWCNT-supported Pd catalysts were synthesized at room temperature using $NaBH_4$ as reducing agent. $(NH_4)_2PdCl_6$ (Stream Chemicals, 99%) was dissolved in deionized water and added to MWCNTs, previously dispersed in water, by continuous ultrasonic stirred for

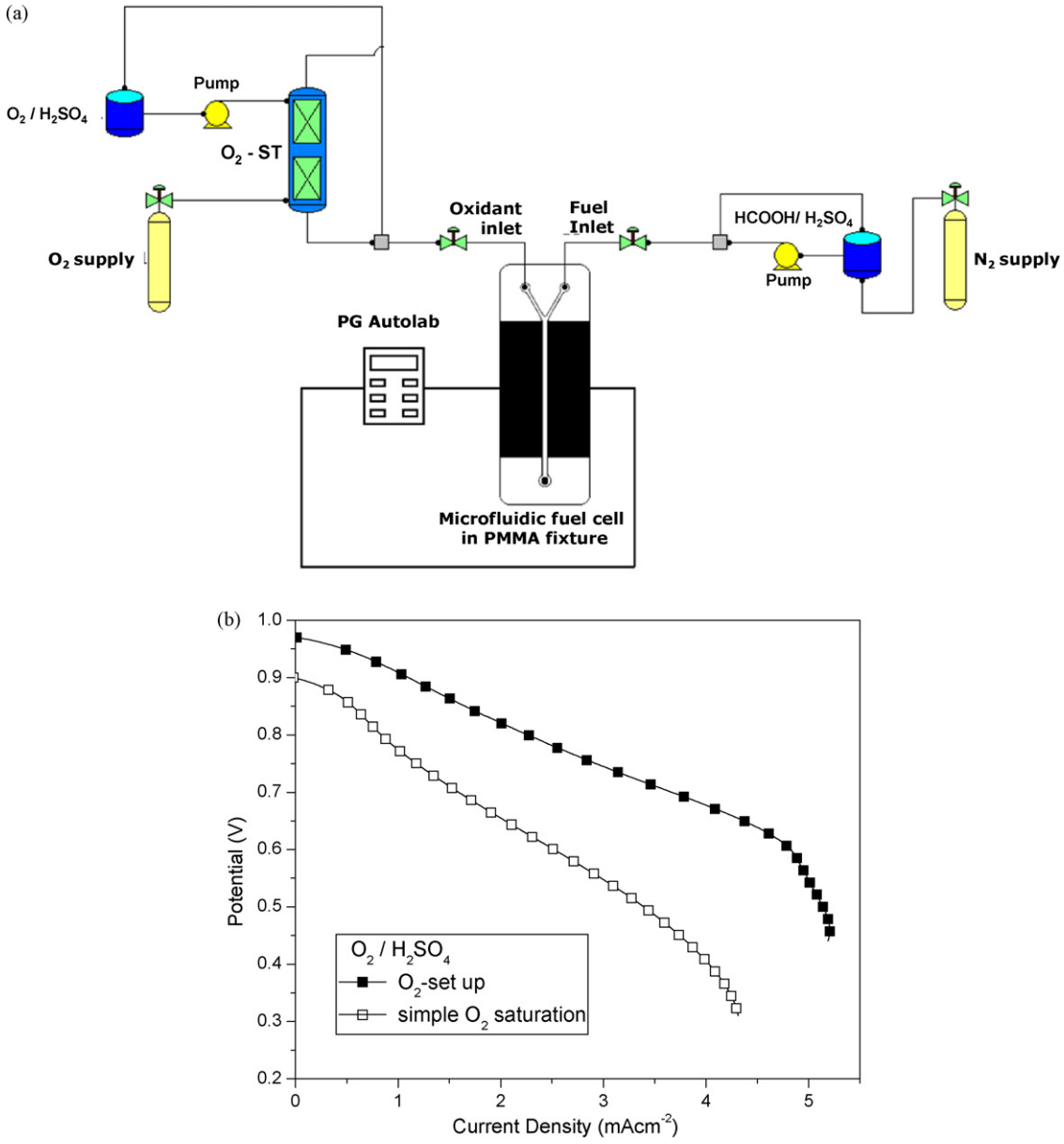

Fig. 2. (a) O_2 saturation acidic fluid setup (O_2-setup) for microfluidic fuel cell evaluation. (b) Polarization curves with Pd/V XC-72 as anode and Pt/V XC-72 as cathode using an O_2-setup in 0.1 M HCOOH at 25 °C under atmospheric pressure.

2 h. $NaBH_4$ (Sigma–Aldrich, 98.5%) was then slowly added to this mixture under vigorous stirring conditions for 1 h. The resulting solution was filtered, washed and dried over night at 60 °C.

2.2. Microfluidic fuel cell development

Cell construction was carried out using the hot-press method, utilizing a PMMA material heated at 140 °C and pressed to 24,000 lbs in.$^{-2}$. The micro-fuel cell dimension is 2 mm width (each channel 1 mm), 1 mm high and 45 mm long with an electrode area of 0.45 cm^2. Anode and cathode current collectors were fabricated using XC72-Vulcan. Electrodes (anode and cathode) were deposited by the spray technique, using an ink prepared with a mixture of nafion, isopropyl alcohol and powders of the electrocatalyst materials. Two micro-fuel cells were constructed in order to compare our synthesized Pd/MWCNTs with the Pd/V XC-72 material. The cathode electrode was maintained in both cells with a loading of 1.9 mg cm^{-2} using Pt/V XC-72 (30 wt.% from E-TEK). Anode electrodes were constructed using Pd/V XC-72 (20 wt.% from E-TEK) and Pd/MWCNTs (12 wt.%) with a Pd loading of 1.3 and 0.7 mg cm^{-2} respectively.

2.3. Microfluidic fuel cell testing setup

Fluid flow in all the fuel cell experiments is pressure driven a regulated using a pump (Masterflex Cole-Palmer Mod-7553-70). In this study, the concentrations of formic acid (88%, Fermont) were chosen as 0.1 and 0.5 M with a flow rate of 0.2 ml min^{-1}. Dissolved oxygen (4.3 U.A.P. Praxair) in 0.5 M H_2SO_4 (97.9%, J.T. Baker) on the other hand, was previously humidified using a saturation tower (O_2-ST) and fed to the cathode with a flow rate of 1.05 ml min^{-1}. Voltage and current measurements were performed utilizing an Autolab Pontenciostat/Galvanostat PGSTAT30. All tests were performed at 25 °C. A schematic representation of the microfluidic fuel cell test apparatus is shown in Fig. 2a.

3. Results and discussion

3.1. Physicochemical characterization

X-ray diffraction patterns collected from Pd/V XC-72 and Pd/MWCNT catalysts are shown in Fig. 1. The highest peak located at 26° corresponds to the graphite plane (0 0 2) of MWCNT support. The other peaks show a face-centered-cubic (fcc) crystallographic structure typical of Pd, corresponding to the planes (1 1 1), (2 0 0), (2 2 0) and (3 1 1). The average crystallite size of the two catalysts was estimated from diffractograms using the Scherrer equation applied to the (2 2 0) peak. In this way, 6 and 4 nm were obtained for Pd/V XC-72 and Pd/MWCNT catalysts respectively.

3.2. Microfluidic fuel cell performance using a Pd/XC-72 anode with and without O_2-ST

Fig. 2b shows polarization curves with Pd/V XC-72 as anode and Pt/V XC-72 as cathode with and without O_2-ST in 0.1 M of HCOOH at 25 °C. Inspection of the obtained results shows that when an O_2-ST is used, the open circuit potential and the maximum current density are increased from 0.9 to 0.97 V and from 4.3 to 5.3 mA cm^2 respectively, probably due to the increase in the oxygen concentration. This explanation relies on the fact that the rashing rings (3/8 in. diameter) contained in O_2-ST must allow an increase in the oxygen contact time with the acidic sulfuric acid fluid. Under this assumption, it is therefore possible to conclude that the microfluidic cell performance is enhanced with the incorporation of the O_2-setup.

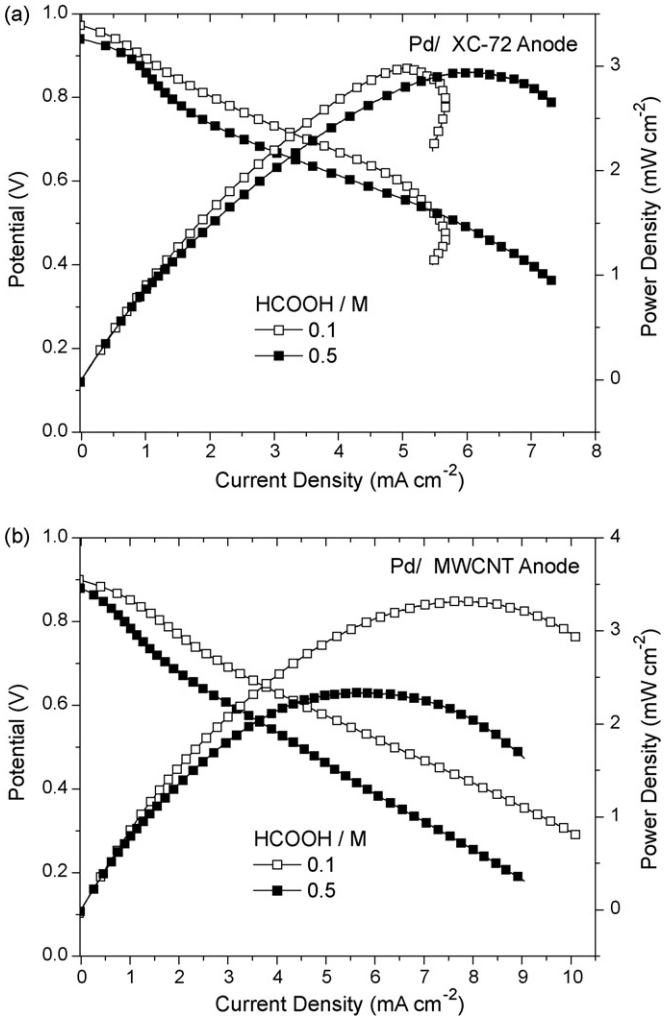

Fig. 3. Polarization and power density curves in 0.1 and 0.5 M HCOOH for the microfluidic fuel cell equipped with (a) Pd/V XC-72 and (b) Pd/MWCNT anode catalysts at 25 °C under atmospheric pressure.

3.3. Pd/V XC-72 and Pd/MWCNT anode electrodes performance

Fig. 3 shows the polarization and power density curves for (a) Pd/V XC-72 and (b) Pd/MWCNT anode electrodes operating under 0.1 M and 0.5 M HCOOH conditions. It is interesting to note that while the open circuit potential in both cases (Fig. 3a and b) remains similar in 0.1 and 0.5 M of HCOOH, the maximum power density does not change for the Pd/V XC-72 anode electrode, and it does change for the Pd/MWCNT anode electrode. In the later case, the HCOOH concentration effect is reflected by a decrement from 3.3 to 2.3 mW cm^{-2} for 0.1 and 0.5 M of HCOOH respectively (Fig. 3b). With the purpose of evaluating under higher HCOOH concentrations, both anode electrodes were evaluated in 1 M HCOOH, observing in this case a decrement in the maximum power densities (data not showed). Under this scenario, it is possible to suggest that at high HCOOH concentrations (>0.1 M), the microfluidic fuel cell performance is limited by slow anode/cathode kinetics, low oxygen concentration or slow diffusion of reagents to the electrode surface, due to the formation of a concentration boundary layer. In addition, the formation of bubbles on the electrode surface, particularly carbon dioxide, could hinder the performance of the microfluidic fuel cell by disturbing the flow pattern. Another interesting observation can be drawn from Fig. 3b, where it is possible to see an increment in the power density value (3.3 mW cm^{-2}) compared to that reached with commercial Pd (2.9 mW cm^{-2}). Comparison of

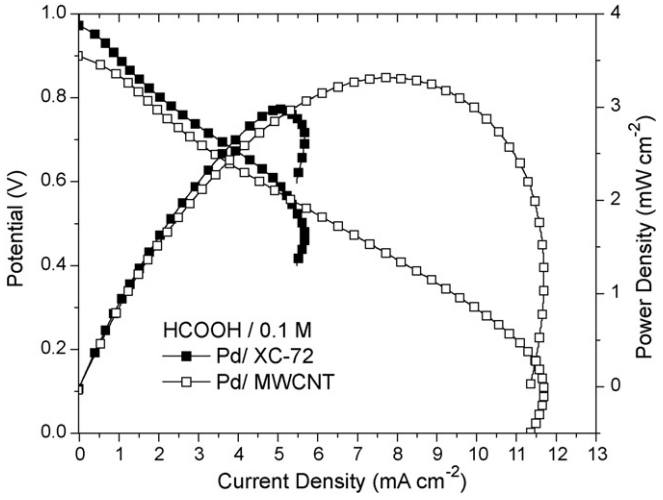

Fig. 4. Polarization and power density curves in 0.1 M HCOOH for the microfluidic formic acid fuel cell equipped with Pd/V XC-72 and Pd/MWCNT anode catalysts at 25 °C under atmospheric pressure.

the microfluidic fuel cell performance in 0.1 M of HCOOH on the other hand, is shown in Fig. 4. The results show that the highest power density (2.9 mW cm^{-2}) previously reported, that uses a commercial Pd/V XC-72 anode electrode [10], is surpassed by a cell utilizing a Pd/MWCNT that is also characterized by 50% less Pd loading (3.3 mW cm^{-2}). The increased power density and less Pd loading could be associated to the use of carbon nanotubes as support, which is known to have better electric properties than those of Vulcan.

4. Conclusions

The incorporation of an O_2 saturation acidic fluid setup (O_2-setup) coupled to the MWCNT-supported Pd nanoparticles as anode electrocatalyst in the microfluidic fuel cell prototype (0.45 cm^2 electrode area) presented in this work, resulted in current densities up to 11 mA cm^{-2} using low formic acid concentrations (0.1 M). The better electric properties of MWCNTs as well as the improved particle distribution on the support material as compared to Vulcan, is believed to result in an increase in the maximum power density up to 3.3 mW cm^{-2}, even when the Pd catalyst loading was 50% less than that of the commercial catalyst Pd/V XC-72. Further studies are being carried out in our laboratory in order to fully understand the different variables that condition the Y-shaped microfluidic fuel cell performance.

Acknowledgment

The authors gratefully acknowledge financial support from the Mexican Council for Science and Technology (CONACyT, Grant 61067).

References

[1] S. Ha, R. Larsen, Y. Zhu, R.I. Masel, Fuel Cells 4 (2004) 337.
[2] M. Baldauf, D.M. Kolb, J. Phys. Chem. 100 (1996) 11375.
[3] M. Tian, B.E. Conway, J. Electroanal. Chem. 581 (2005) 176.
[4] N. Hoshi, K. Kida, M. Nakamura, M. Nakada, K. Osada, J. Phys. Chem. B 110 (2006) 12480.
[5] W.P. Zhou, A. Lewera, R. Larsen, R.I. Masel, P.S. Bagus, A. Wieckowski, J. Phys. Chem. B 110 (2006) 13393.
[6] S. Ha, R. Larsen, R.I. Masel, J. Power Sources 144 (2005) 28.
[7] X. Wang, W. Li, Z. Chen, M. Waje, Y. Yan, J. Power Sources 158 (2006) 154–159.
[8] S. Yang, X. Zhang, H. Mi, X. Ye, J. Power Sources 175 (2008) 26–32.
[9] D. Morales-Acosta, J. Ledesma-Garcia, Luis A. Godinez, H.G. Rodriguez, L. Alvarez-Contreras, L.G. Arriaga, J. Power Sources 195 (2010) 461–465.
[10] E. Kjeang, N. Djiali, D. Sinton, J. Power Sources 186 (2009) 353–369.
[11] R. Ferrigno, A.D. Stroock, T.D. Clark, M. Mayer, G.M. Whitesides, J. Am. Chem. Soc. 124 (2002) 12930–12931.
[12] E.R. Choban, L.J. Markoski, A. Wieckowski, P.J.A. Kenis, J. Power Sources 128 (2004) 54–60.
[13] R.S. Jayashree, L. Gancs, E.R. Choban, A. Primak, D. Natarajan, L.J. Markoski, P.J.A. Kenis, J. Am. Chem. Soc. 127 (2005) 16758–16759.
[14] A. Li, S.H. Chan, N.T. Nguyen, J. Micromech. Microeng. 17 (2007) 1107–1113.
[15] J.L. Cohen, D.A. Westly, A. Pechenik, H.D. Abruna, J. Power Sources 139 (2005) 96–105.
[16] V. Baglio, A. Di Blasi, C. D'Urso, V. Antonucci, A.S. Aricò, R. Ornelas, D. Morales-Acosta, J. Ledesma-Garcia, L.A. Godinez, L. Alvarez-Contreras, L.G. Arriaga, J. Electrochem. Soc. 155 (2008) B829–B833.